Published in final edited form as:
Magn Reson Imaging. 2008 December ; 26(10): 1352–1359. doi:10.1016/j.mri.2008.04.010.

Quantification of Cerebral Perfusion Using the "Bookend Technique": an Evaluation in CNS Tumors

Timothy J Carroll, **Sandra Horowitz**, **Wanyong Shin**, **Jessy Mouannes**, **Rahul Sawlani**, **Saad Ali**, **Jeffrey Raizer**, and **Stephen Futterer**

Abstract

We present a method of quantifying cerebral blood volume using Dynamic Susceptibility Contrast. Our approach combines T2-weighted EPI pulse sequences and reference scans that determine the parenchymal T1-changes resulting from an injection of a gadolinium chelate. This combined T2-and T1-weighted approach (The "Bookend" technique) has been shown to be effective in the quantification of Gradient-Echo (T2*-weighted) perfusion images, but has not been applied to Spin –Echo EPI (T2-weighted) images. The physics related to blood volume measurement based on T2- and T2*-weighted EPI sequences is known to be different, and there is a question as to whether the bookend approach is effective with SE-EPI. We have compared the quantitative SE-EPI with GE-EPI in a series of patients with central nervous system (CNS) tumors. We found that quantitative cerebral Blood Volume (qCBV) values for SE-EPI and GRE-EPI are in agreement with each other and with historical reference values. A subjective evaluation of image quality showed that image quality in the SE-EPI scans was high and exhibited high inter-reader agreement. We conclude that measuring qCBV using the bookend technique with SE-EPI images is possible and may be a viable alternative to GRE-EPI in the evaluation of CNS tumors.

Introduction

We report on the development of an image protocol capable of quantification of cerebral perfusion with Spin-Echo MRI images. Cerebral perfusion images are commonly calculated from dynamic susceptibility contrast (DSC) images and deconvolution analysis of the time course of contrast agent bolus (1–4). Perfusion weighted MR imaging has found widespread use in a variety of neurovascular and oncological diseases (5–12). Both T2*-weighted Gradient echo EPI (GRE-EPI) and T2-weighted Spin-echo (SE-EPI) measures of relative cerebral blood volume have been used to identify cerebral blood volume changes related to tumor angiogenesis (5–8,10,13). In particular, relative cerebral blood volume (rCBV), which is calculated as the integrated concentration-time curve, has been shown to correlate with tumor grade in primary Central Nervous System (CNS) tumors (11). Currently, relative CBV (rCBV) tumor evaluation is compared to normal contralateral White Matter (WM) as a reference to quantify tumor blood volume changes. A means to set an absolute scale (i.e. report CBV in ml/100g of tissue) would allow for direct scan-to-scan changes in tumor blood volume. With the advent of angiogenic inhibiting drugs there is interest in developing protocols for absolute quantification of cerebral blood volume as a means to track changes that are associated with tumor regression. Absolute quantification will allow comparison of intra- and inter-patient blood volume changes throughout the treatment of a CNS tumor with angiogenic inhibitors.

Since CBV is the perfusion parameter normally associated with CNS tumor angiogenesis we have focused this analysis on CBV quantification rather than cerebral blood flow (CBF) or mean transit time (MTT). GRE-EPI blood volume images are prone to overwhelming signal from the artifactual "blooming" of large blood vessels (14,15) which are less of a problem with SE-EPI images. However, since SE-EPI images carry less susceptibility weighting than GRE-EPI acquisitions (14,15) SE-EPI are less sensitive to blood vessels which are larger than 10 μm. The lack of sensitivity to larger blood vessels in SE-EPI results in a systematic underestimation of CBV. Due to the lack of sensitivity to larger blood vessels, there is a question as to whether quantification of CBV is possible with SE-EPI. The quantification of CBV is also complicated by partial volume averaging of arteries, transient T1-changes during first pass of the bolus as well as non-linearities in signal response at high concentrations. These combined effects make the quantification of cerebral blood volume with SE-EPI challenging.

A technique to reliably quantify cerebral perfusion with a GRE-EPI acquisition has been reported (16–18). This approach is based on calibration of relative perfusion images based on T1-weighted pre-and post-gadolinium reference scans and has been evaluated through direct comparison with microsphere measurement of perfusion(19). These reference scans are performed on both sides of the GRE-EPI scan as "bookends". The bookend scans quantify the parenchymal T1 changes, the blood pool T1-changes and are used to correct for intravascular-to-extravascular water exchange. To date the bookend technique has only been evaluated as a means of quantifying perfusion using GRE-EPI acquisitions.

We report on a novel MR imaging protocol that quantifies CBF (qCBF) and CBV (qCBV) using a SE-EPI acquisition. This protocol was evaluated in patients with pathologically confirmed, primary CNS tumors. Our quantitative blood volume imaging protocol combines: parallel imaging (20–22) to reduce the echo time of a multi-phase SE-EPI perfusion scan, the bookend technique (16) to quantify perfusion, and an algorithm to correct for intra-vascular to-extravascular water exchange (17). We compared the results to quantitative GRE-EPI perfusion as a reference standard (16,17,23) and performed both qualitative and quantitative analysis of perfusion images. We report, for the first time, quantitative values of CBV (ml/100g) in pathologically confirmed low grade (World Health Organization (WHO) Grade II) and high grade (WHO Grade IIII, IV) gliomas using DSC MRI.

Materials and Methods

Patients and volunteers were scanned on a clinical 1.5T MRI scanner (Avanto, Esprit Siemens Medical Systems) with both GRE-EPI and SE-EPI perfusion acquisitions in this HIPAA compliant study that was approved by the institutional review board at our institute. All image processing and analysis was performed using commercially available software (MATLAB 6.5, Mathworks, Inc., Matick, MA).

Cerebral Blood volume Quantification

The quantification of CBV was based on the bookend technique(16) which determine CBV from T1 changes in normal white matter in relation to the changes in the blood pool(24,25). This approach relies on careful modeling of the effects of intravascular to extravascular water exchange (17), which is a well-known confounding effect in determining CBV from pre-and post gadolinium T1-changes(26). The quantification of blood volume is calculated from the T1 changes in white matter and the blood pool as:

$$CBV_{ss} = WCF \times \frac{K_H}{\rho} \frac{[1/T_1{}^{pre-contrast} - 1/T_1{}^{post-contrast}]_{WM}}{[1/T_1{}^{pre-contrast} - 1/T_1{}^{post-contrast}]_{BloodPool}} \times (100g/ml) \quad [1]$$

Where ρ is the average density of a brain (1.04 ml/g) and K_H (0.74) is a dimensionless constant which corrects for the hematocrit between capillaries and arteries (27). The T1 of blood in the sagittal sinus was used as the T1 of blood and an ROI was draw to cover normal appearing White Matter (WM). The Water Correction factor (WCF) is a dimensionless constant that accounts for the intra-vascular to extra-vascular water exchange (17), which is known to be a confounding effect in calculation of qCBV based on T1-changes (17,28,29). The WCF depends on tissue type, but varies little in the expected ranges of normal white matter and can be parameterized as:

$$WCF(\Delta R1)=8.2\times 10^{-3}\Delta R1^{2}+0.25\Delta R1+0.51 \quad [2]$$

Eq. (2) is valid in white matter at 1.5T where ΔR1 is the T1 change of the blood resulting form the gadolinium injection. QCBF values were derived from the qCBV values using the deconvoled MTT images and the central volume principle (CBF= CBV/MTT).

Image Acquisition

Patient Studies—The parameters for the GRE-EPI and SE-EPI acquisitions were as follows: Field of view (FOV)=220×220mm, matrix = 128×128, TR=1290ms, 13–15 slices, slice thickness/the gap between slices=5mm/1.5mm, bandwidth=1260 Hz/pixel, TE (GRE/SE) = 47ms/60ms, tip angle=90°. The SE-EPI were acquired using parallel imaging (acceleration factor=2, reference lines=24) using GRAPPA reconstruction (22). The DSC perfusion images were acquired with a Gadolinium based contrast agent (Magnevist, Berlex, Princeton) injected with a power injector (Spectris, Medrad, Indiana, PA) at a rate of 4 ml/sec followed by a 15 ml saline flush at 4 ml/sec. GRE-EPI images were acquired prior to SE-EPI images in all cases. In this retrospective feasibility study, randomization of acquisition order was not possible. The contrast agent injection associated with the initial GRE-EPI scan served as a preloading contrast dose. The use of preloading contrast injections is common in SE-EPI perfusion scans to mitigate the signal changes associated with T1 shortening, which can offset signal changes resulting from transient T2 changes. The injection protocol for the examination was: 60% of single dose of contrast (0.06 mmol/kg) was injected for the GRE-EPI images, and subsequently, a single dose (0.1 mmol/kg) was injected for the SE-EPI acquisition at the same injection rate rate.

For the calculation of perfusion from the DSC images, the arterial input function (AIF) was chosen automatically (30) to reduce operator error and streamline post processing of the perfusion data. Singular value decomposition was used to deconvolve the AIF (3) and produce the standard set of perfusion weighted images: rCBV, rCBF, and Mean Transit Time (MTT).

For the bookend reference scans we used a segmented Inversion Recovery (IR) Look-Locker (31) echo planar pulse sequence (LL-EPI), TR/TE= 21/9.9ms, 128×128 matrix, 220 mm field of view, 21 lines in k-space per an acquisition, 5 mm thickness, 120 time points, scan time 45 sec) to measure T1 changes WM and the blood pool (See Eq. (1)). A region of interest (ROI) was drawn contra-lateral to the glioma to determine CBV in normal appearing WM using standard techniques(7). As with the AIF selection, WM ROI in the bookend analysis was also chosen automatically based on the distribution of T1 values in the LL-EPI images (17). The value of qCBVss determines the quantitative scale of normal appearing white matter and is applied globally to rCBV image to yield whole brain qCBV maps and subsequently qCBF images.

Qualitative Analysis

Twenty-two consecutive patients (13 male, 9 female; age range, 33 – 74 years; mean age, 50.5 years) referred to the Department of Radiology for pre-operative assessment of intra-axial brain tumors between April 2005 and Feb 2006 were retrospectively studied. Quantitative MR CBV

exams with both GE- and SE-EPI techniques were obtained for each patient during the same procedure to allow an exact comparison of the findings.

Color maps of qCBV were printed with 9 images on 1 page (two pages per exam). In all cases a common image scale was used (0.0 – 4.0 ml/00g) so that normal deep WM corresponds to the middle of the color range. Images were randomized in order so that SE-EPI and GRE-EPI images from the same patient fell randomly in the list of 44 exams. A blinded independent review was performed by two board-certified neuroradiologists (,) of the forty-four exams (22 of GRE and 22 of SE) obtained from twenty-two patients. The readers were asked to evaluate and grade the image quality on a four-point scale (0–3) for four characteristics. The grading system used to assess the perfusion images was as follows:

1. signal dropout near the frontal/ethmoid sinuses: 0-none, 1-mild, 2-moderate, or 3-severe signal loss
2. signal dropout near the internal auditory canal: 0-none, 1-mild, 2-moderate, or 3-severe signal loss
3. the level of vessel “blooming” from the cortical blood vessels: 0-vessels visible in sulci, 1-vessels appear large and obscure the cortical gray matter (GM), 2-uninterpretable perfusion in the cortical ribbon but interpretable in adjacent subcortical WM, 3-large vessel artifact overwhelming enough to bias CBV in adjacent subcortical WM
4. operator subjective diagnostic confidence of the perfusion images: 0-high quality images with highest diagnostic confidence, 1-moderate confidence because of artifact or signal loss, 2-poor images with low diagnostic confidence, and 3-uninterpretable images

The readers were also allowed to mark an ‘x’ in lieu of a numeric value in cases where the anatomic coverage of the images was insufficient to evaluate the category. For example if the coverage was insufficient and did not include the internal auditory canal, evaluation of signal dropout in this area would have been impossible. Prior to this review, a separate set of 12 exams served as “training data” and were reviewed in consensus by the two observers using identical scoring system.

The scores provided by the two reviewers were tabulated. The strength of inter-observer agreement was assessed by means of quadratically-weighted Cohen’s Kappa statistic. Results from both readers were averaged to create mean score for each metric of image quality. The means were then averaged over each patient. A paired Student’s t-test was performed on the composite score to determine whether there was significant difference between the image quality in the GRE-and SE-EPI images. Significant difference was defined at the 5 % level.

Volunteer Studies—In order to isolate the improvements seen the in the SE-EPI images afforded by the use of parallel imaging we performed an ancilliary study in healthy volunteers. A series of 5 volunteers were scanned using a slightly modified scan protocol. In this study, the TR, TE and parallel imaging parameters or both perfusion acquisitions were matched (TR/TE=1500 ms/61 ms, acceleration factor=2, reference lines=24), all other image parameters were identical to the patient studies (FOV/Matrix = 220 mm/128, tip angle=90°, 13 slices, bandwidth=1260 Hz/pixel) LL-EPI scans were performed before and after the EPI perfusion scans. The SE- and GRE images were evaluated in separate blinded reads identical to the reads performed in the patient studies. As with the patient studies, scores were pooled across reader, and subject and the mean values were compared using a Student’s t-test with significance defined at the 5% level.

Quantitative Analysis

A paired comparison of quantitative CBV (qCBV) and quantitative CBF (qCBF) values from GRE- and SE-EPI perfusion was performed to evaluate the bookend technique in a patient population. An independent ROI analysis of the patients studied was performed by a resident physician (). ROIs were drawn contralateral to the lesion remote from the craniotomy or radiation effect. A total of 3 patients were rejected based on poor image quality which would affect our ability to define "normal" WM and GM ROIs (EPI distortion n=2, extensive radiation damage n=1). This resulted in a total of 19 subjects in which both GRE-EPI and SE-EPI scans were interpretable. WM ROIs were drawn in the mid-lateral ventricular and frontal white matter. GM ROIs were draw to cover cortical GM. Mean values and standard deviations were compared to test the hypothesis that quantitative CBV and CBF in SE-EPI are significantly different. Significance was determined at the 5% level. Correlation and Bland-Altman analyses were performed to elucidate qCBV and qCBF dependent trends.

Finally, an analysis of tumor perfusion in a sub-sample of pathologically confirmed infiltrative gliomas (N=13, 3 female, 11 male, <age>=53, range 32–73 years) was conducted. Subsequent histopathology confirmed 6 low-grade gliomas that included two WHO Grade II Oligodendrogliomas and four WHO Grade II Mixed Oligoastrocytomas (MOA). Seven high-grade gliomas included four Glioblastoma Multiforme (GBM), one GBM mixed with gliosarcoma, one Anaplastic Astrocytoma III, and one grade III MOA. In these patients, tumor perfusion was evaluated with the standard rCBV images using normal contralateral WM as a reference and using the qCBV maps. The regions of interest drawn in the rCBV images were automatically propagated to the qCBV images to provide blinding of the quantitative results. The GRE-EPI and SE-EPI images of qCBV were evaluated. Tumor perfusion was determined manually as described below.

A neuroradiologist () with over 20 years experience in brain tumors performed a ROI analysis on the qCBV images, blinded to the quantitative results. Local perfusion was evaluated by placing an ROI over the enhancing portion of the tumor using the post-gadolinium T1 weighted anatomical scans as a guide. Reference ROIs were placed in contralateral normal appearing WM by the same operator using a previously reported technique (6–8,10,11). The mean value of WM, GM, low grade (WHO grade II) and high grade (WHO grades III, IV) were compared. Tumor progression defined as neurological degeneration or 25% growth in size has been shown to correlate with a local increase in tissue perfusion as measured by the ratio of tumor perfusion to contralateral normal WM (11).

Results

MRI Imaging was successful in all cases and no adverse events were reported.

Qualitative Analysis

Figure 1 shows a representative paired comparison between qCBV images acquired with GRE- and SE-EPI images. Image artifacts from cortical blood vessels are more pronounced on the GRE-EPI images and in many regions of the cerebral cortex. Conversely, the signal dropout in the vicinity of the frontal sinuses is greatly reduced on the SE-EPI images. There were 12 perfusion studies which did not cover the internal auditory canal (marked with an 'x' by the reviewers) and were, therefore, excluded in our subsequent analysis.. Results of the qualitative analysis are shown in graphically in Figure 2, and are reported in Table 1. On average, the GRE-EPI images were found to have a higher level of artifact than the SE-EPI images in all three areas where they were evaluated. In two of the three categories (Frontal sinuses and "vessel blooming" artifact), the differences were found to be statistically significant. Diagnostic confidence was found to be significantly higher in the SE-EPI images ($p<0.05$). In

the evaluation of signal dropout in the region surrounding the internal auditory canal, the SE-EPI suffered from less artifact; however, the improvement was not statistically significant ($p<0.21$). Interobserver agreement was high for evaluation of artifact, but only "good" for the diagnostic confidence. We found κ-values of 0.66, 0.68, 0.79 and 0.50 for frontal sinus artifact, auditory canal artifact, vessel blooming artifact and diagnostic confidence, respectively (See Table 1).

The ancillary volunteer study of GRE and SE with the effects of echo time and parallel imaging removed supported the findings of the patient studies. We observe statistically significant reduction in the frontal sinus artifact (mean scores for GRE/SE were 0.15 ± 0.22/1.65 ± 0.14, $P<10^{-5}$), vessel blooming (mean scores for GRE/SE were 0.10 ± 0.14/1.40 ± 0.45, $P<0.005$) and improved diagnostic confidence (mean scores for GRE/SE were 0.15 ± 0.22/1.40 ± 0.38, $P<0.004$). Due to the scan prescription, which did not include the internal auditory canals in all scans, a rigorous statistical analysis was not possible. However, a trend toward less artifact in the SE scans (mean score 1.38 compared to 1.0 for GRE) was observed.

Quantitative Analysis

The mean values of qCBV and qCBF for WM and GM are reported in Table 2 for SE-EPI and GRE-EPI separately. We found that there was a significant difference in qCBV measured in GM ($p<0.03$), but there were no significant differences between any other measure of perfusion. Scatter plots of qCBF and qCBV are shown in Figure 3. SE-EPI and GRE-EPI values for qCBV and qCBF were found to be highly correlated (Figures 3(a) and 3(c), $r=0.77$, $p < 10^{-10}$ and $r= 0.82$, $p< 10^{-08}$ for qCBV and qCBF respectively). The Bland-Altman analysis showed a bias (sigma) of −0.12 ± 0.37 ml/00g in the qCBV (Figure 3b) comparison and a bias (sigma) of 2.95 ± 11.03 ml/100g-min for qCBF (Figure 3d).

A representative comparison of SE-EPI and GRE-EPI in a high grade (WHO grade IV) is shown in Figure 4. These images from a 52 year old male with a pathologically confirmed "butterfly" GBM show elevated qCBV throughout the right frontal mass and genu of corpus callosum. Increased CBV at the peripheral rim of the tumor and central necrosis showing decreased qCBV is also evident.

Both quantitative and relative CBV values were compared in the sample of low and high grade gliomas (See center top). SE-EPI shows less patient-to-patient variability in the measurement of normal WM and, consequently, in the relative values of tumor perfusion. Because GRE-DSC CBV is sensitive to susceptibility effects from total vascular beds, including large vessels, the normal arteries and veins located at the cortical sulci near the surface of brain or immediately periventricular may be misinterpreted as tumor vascularity. The mean, standard deviation of low and high grade gliomas is reported in Table 3. We report tumor perfusion from GRE-EPI and SE-EPI separately. We found that our values for intra-tumoral rCBV to be consistent with previously reported results.

Discussion

We report, for the first time, the quantitative value of CBV in low- and high grade gliomas as measure with DSC MRI. We found that SE-EPI produces comparable values for cerebral perfusion as the more established GRE-EPI images, with significantly less image artifact. Quantitative MR CBV images acquired with a SE-EPI pulse sequence were found to be of higher quality than GRE-EPI images. These finding suggest that parallel imaging combined with SE-EPI perfusion images could be a useful component of a comprehensive neuroradiolgical examination in the evaluation of gliomas.

We measured qCBF and qCBV in WM and GM (Table 3) and found that qCBV and qCBF in WM and GM to be agreement with previously report values for cerebral perfusion using radiolabelled positron emission tomography (PET) imaging. Cerebral perfusion measurement using PET are: qCBF=24.7 ± 5.3 ml/100g-min 47.4 ± 3.85ml/100g-min for WM/GM; qCBV = 1.91 ± 0.62 ml/100g/3.85 ± 0.58 ml/100g for WM/GM (32,33). A key difference between PET and MRI perfusion images is that PET does not rely on the existence of an intact blood brain barrier and is not prone to field inhomogenity effects. This represents a clear advantage over MR imaging for the imaging of GM perfusion, where cortical blood vessels can confound the accurate measurement of capillary level blood flow. However, radiolabelled-water PET perfusion images are much lower in spatial resolution and requires an on-site cyclotron due to the short half-life of $H_2[O^{15}]$ tracer, which limits its availability. One goal of this SE-EPI technique was to reduce the effect for large vessels in the region where cortical GM dominates. We found that it is possible to measure GM perfusion (See Figure 1), but careful ROI selection by a trained operator is needed.

A subjective qualitative analysis showed that our SE-EPI imaging protocol outperformed GRE-EPI scans. This is in agreement with prior comparisons of SE-EPI and GRE-EPI. We have found that our combined T1- and T2-wighted scan protocol does not compromise SE-EPI image quality. Our qualitative analysis was based upon blinded independent reads. The inter-reader agreement further supports our hypothesis that image quality is improved with SE-EPI.

SE-EPI acquisitions are used less frequently that GRE-EPI due to requirement of a time-consuming additional 180° refocusing pulse. The use of parallel imaging was a key component to the SE-EPI imaging protocol. This allows SE-EPI scan parameters (TR/coverage/resolution) to be closely matched to those of the GRE-EPI, allowing direct comparison. Parallel imaging is well established as a method of accelerating images acquisitions and is standard on many MRI systems. Parallel imaging acceleration is normally used to reduce imaging time. We were able to use parallel imaging to reduce the echo time, and subsequently the repetition time of a SE-EPI acquisition. Rather that reducing the total scan time, we exploited parallel imaging to maintain the superior/inferior coverage that is possible in GRE-EPI scans. SE-EPI perfusion scans are normally limited in the number of slices per TR that can be acquired, and subsequently the coverage. In CNS tumor imaging it may be possible to cover most primary gliomas with 3–5 5.0 mm slices, however the limitation can be problematic for larger lesions. The reduction of echo time, was also a contributor to the improved image quality and improved visualization of the gray matter in the cortex. These effects were reflected in the higher qualitative scores.

Sugahara et al (13) compared relative CBV in high grade gliomas to low grade gliomas with GRE-EPI and SE-EPI. Our results (Table 3) from rCBV agree with their findings (GRE = 5.0 ± 2.9, SE-EPI = 2.9 ± 2.3). For low grade gliomas, they report rCBV values of 1.2±0.7 and 1.2 ± 0.6 for high and low grade tumors, respectively. The Sugahara et al (13) results are consistent with a recent study by Law et al (11), who found that tumors with an rCBV of less than 1.75 are less likely to progress (i.e are low grade) than those with higher rCBV. We see a similar trend. But with the additional information provided by quantification and with a larger data set we may have the ability to determine an absolute scale factor for the stratification of angiogenically induced CBV changes.

This study is not without limitations. We have compared GRE-EPI and SE-EPI quantitative CBV, but due to the limited scope of this technical note, additional imaging studies with a suitable standard of reference (i.e. $H_2[O^{15}]$ PET), were impossible. Furthermore, many of these patients were scanned immediately prior to surgical intervention, further complicating the access to additional image studies that would allow for a standard of reference. Our imaging protocol acquired GRE-EPI perfusion images prior to SE-EPI images in all cases. This was intentional so that the injection required for the GRE-EPI images served as a preloading dose

for the SE-EPI images. The use of a pre-loading dose to improve SE-EPI perfusion images is common and is know to mitigate T1-leakage effects in tumors with compromised blood-brain barriers. However, in this study it precluded randomization of image acquisition order. Finally, the bookend technique currently required two separate 45 second scans to be performed. Although this implementation is cumbersome, there have been reports of a pulse sequences that can eliminate the additional scans (34).

In conclusion, we have found that the application of the T1-bookend method of quantification to SE-EPI has shown that high quality quantitative perfusion weighted images are possible. A direct comparison of GRE-EPI and SE-EPI images has shown that quantitative cerebral blood volume values are highly correlated. A qualitative analysis has showed that this technique for quantification results in quantifiably higher image quality along with high inter-reader agreement.

References

1. Rosen BR, Belliveau JW, Vevea JM, Brady TJ. Perfusion imaging with NMR contrast agents. Magn Reson Med 1990;14(2):249–265. [PubMed: 2345506]
2. Rosen BR, Belliveau JW, Aronen HJ, Kennedy D, Buchbinder BR, Fischman A, Gruber M, Glas J, Weisskoff RM, Cohen MS, et al. Susceptibility contrast imaging of cerebral blood volume: human experience. Magn Reson Med 1991;22(2):293–299. [PubMed: 1812360]discussion 300–293
3. Ostergaard L, Weisskoff RM, Chesler DA, Gyldensted C, Rosen BR. High resolution measurement of cerebral blood flow using intravascular tracer bolus passages. Part I: Mathematical approach and statistical analysis. Magn Reson Med 1996;36(5):715–725. [PubMed: 8916022]
4. Ostergaard L, Sorensen AG, Kwong KK, Weisskoff RM, Gyldensted C, Rosen BR. High resolution measurement of cerebral blood flow using intravascular tracer bolus passages. Part II: Experimental comparison and preliminary results. Magn Reson Med 1996;36(5):726–736. [PubMed: 8916023]
5. Pathak AP, Schmainda KM, Ward BD, Linderman JR, Rebro KJ, Greene AS. MR-derived cerebral blood volume maps: issues regarding histological validation and assessment of tumor angiogenesis. Magn Reson Med 2001;46(4):735–747. [PubMed: 11590650]
6. Law M, Yang S, Wang H, Babb JS, Johnson G, Cha S, Knopp EA, Zagzag D. Glioma grading: sensitivity, specificity, and predictive values of perfusion MR imaging and proton MR spectroscopic imaging compared with conventional MR imaging. AJNR Am J Neuroradiol 2003;24(10):1989–1998. [PubMed: 14625221]
7. Cha S. Perfusion MR imaging of brain tumors. Top Magn Reson Imaging 2004;15(5):279–289. [PubMed: 15627003]
8. Law M, Yang S, Babb JS, Knopp EA, Golfinos JG, Zagzag D, Johnson G. Comparison of cerebral blood volume and vascular permeability from dynamic susceptibility contrast-enhanced perfusion MR imaging with glioma grade. AJNR Am J Neuroradiol 2004;25(5):746–755. [PubMed: 15140713]
9. Schmainda KM, Rand SD, Joseph AM, Lund R, Ward BD, Pathak AP, Ulmer JL, Badruddoja MA, Krouwer HG. Characterization of a first-pass gradient-echo spin-echo method to predict brain tumor grade and angiogenesis. AJNR Am J Neuroradiol 2004;25(9):1524–1532. [PubMed: 15502131]
10. Cha S, Tihan T, Crawford F, Fischbein NJ, Chang S, Bollen A, Nelson SJ, Prados M, Berger MS, Dillon WP. Differentiation of Low-Grade Oligodendrogliomas from Low-Grade Astrocytomas by Using Quantitative Blood-Volume Measurements Derived from Dynamic Susceptibility Contrast-Enhanced MR Imaging. AJNR Am J Neuroradiol 2005;26(2):266–273. [PubMed: 15709123]
11. Law M, Oh S, Babb JS, Wang E, Inglese M, Zagzag D, Knopp EA, Johnson G. Low-grade gliomas: dynamic susceptibility-weighted contrast-enhanced perfusion MR imaging--prediction of patient clinical response. Radiology 2006;238(2):658–667. [PubMed: 16396838]
12. Boxerman JL, Schmainda KM, Weisskoff RM. Relative cerebral blood volume maps corrected for contrast agent extravasation significantly correlate with glioma tumor grade, whereas uncorrected maps do not. AJNR Am J Neuroradiol 2006;27(4):859–867. [PubMed: 16611779]

13. Sugahara T, Korogi Y, Kochi M, Ushio Y, Takahashi M. Perfusion-sensitive MR imaging of gliomas: comparison between gradient-echo and spin-echo echo-planar imaging techniques. AJNR Am J Neuroradiol 2001;22(7):1306–1315. [PubMed: 11498419]

14. Weisskoff RM, Zuo CS, Boxerman JL, Rosen BR. Microscopic susceptibility variation and transverse relaxation: theory and experiment. Magn Reson Med 1994;31(6):601–610. [PubMed: 8057812]

15. Sorensen, AG.; Reimer, P. Principles and Current Applications. Georg Thieme Verlag; 2000. Cerebral Perfusion Imaging.

16. Sakaie KE, Shin W, Curtin KR, McCarthy RM, Cashen TA, Carroll TJ. Method for improving the accuracy of quantitative cerebral perfusion imaging. J Magn Reson Imaging 2005;21(5):512–519. [PubMed: 15834910]

17. Shin W, Cashen TA, Horowitz SW, Sawlani R, Carroll TJ. Quantitative CBV measurement from static T1 changes in tissue and correction for intravascular water exchange. Magn Reson Med 2006;56 (1):138–145. [PubMed: 16767742]

18. Shin W, Horowitz SW, Ragin A, Chen Y, Walker MT, Carroll TJ. Quantiative Cerebral Perfusion Using MRI Imaging: An Evaluation of Reproducibility and Age Dependence. Magn Reson Med. 2007(in press)

19. Shin, W.; Ali, S.; Bhatt, H.; Shaibani, A.; Carroll, TJ. Quantitative Cerebral Blood Flow Measurement in a Canine Stroke Model: Validation with Regional Blood Flow Measurement Using Flourescent Microspheres. Berlin, Germany: 2007 May. p. 590

20. Sodickson DK, Manning WJ. Simultaneous acquisition of spatial harmonics (SMASH): fast imaging with radiofrequency coil arrays. Magn Reson Med 1997;38(4):591–603. [PubMed: 9324327]

21. Pruessmann KP, Weiger M, Scheidegger MB, Boesiger P. SENSE: sensitivity encoding for fast MRI. Magn Reson Med 1999;42(5):952–962. [PubMed: 10542355]

22. Griswold MA, Jakob PM, Heidemann RM, Nittka M, Jellus V, Wang J, Kiefer B, Haase A. Generalized autocalibrating partially parallel acquisitions (GRAPPA). Magn Reson Med 2002;47 (6):1202–1210. [PubMed: 12111967]

23. Shin W, Horowitz S, Ragin A, Chen Y, Walker M, Carroll TJ. Quantitative cerebral perfusion using dynamic susceptibility contrast MRI: evaluation of reproducibility and age- and gender-dependence with fully automatic image postprocessing algorithm. Magn Reson Med 2007;58(6):1232–1241. [PubMed: 17969025]

24. Moseley ME, Chew WM, White DL, Kucharczyk J, Litt L, Derugin N, Dupon J, Brasch RC, Norman D. Hypercarbia-induced changes in cerebral blood volume in the cat: a 1H MRI and intravascular contrast agent study. Magn Reson Med 1992;23(1):21–30. [PubMed: 1734180]

25. Kuppusamy K, Lin W, Cizek GR, Haacke EM. In vivo regional cerebral blood volume: quantitative assessment with 3D T1-weighted pre- and postcontrast MR imaging. Radiology 1996;201(1):106–112. [PubMed: 8816529]

26. Kim YR, Rebro KJ, Schmainda KM. Water exchange and inflow affect the accuracy of T1-GRE blood volume measurements: implications for the evaluation of tumor angiogenesis. Magn Reson Med 2002;47(6):1110–1120. [PubMed: 12111957]

27. Rempp KA, Brix G, Wenz F, Becker CR, Guckel F, Lorenz WJ. Quantification of regional cerebral blood flow and volume with dynamic susceptibility contrast-enhanced MR imaging. Radiology 1994;193(3):637–641. [PubMed: 7972800]

28. Hazlewood CF, Chang DC, Nichols BL, Woessner DE. Nuclear magnetic resonance transverse relaxation times of water protons in skeletal muscle. Biophys J 1974;14(8):583–606. [PubMed: 4853385]

29. Donahue KM, Weisskoff RM, Chesler DA, Kwong KK, Bogdanov AA Jr, Mandeville JB, Rosen BR. Improving MR quantification of regional blood volume with intravascular T1 contrast agents: accuracy, precision, and water exchange. Magn Reson Med 1996;36(6):858–867. [PubMed: 8946351]

30. Carroll TJ, Rowley HA, Haughton VM. Automatic calculation of the arterial input function for cerebral perfusion imaging with MR imaging. Radiology 2003;227(2):593–600. [PubMed: 12663823]

31. Look DC, Locker DR. Time Saving in Measurement of NMR and EPR Relaxation Time. Rev Sci Intrum 1970;41(2):250–251.

32. Frackowiak RS, Lenzi GL, Jones T, Heather JD. Quantitative measurement of regional cerebral blood flow and oxygen metabolism in man using 15O and positron emission tomography: theory, procedure, and normal values. J Comput Assist Tomogr 1980;4(6):727–736. [PubMed: 6971299]

33. Pantano P, Baron JC, Lebrun-Grandie P, Duquesnoy N, Bousser MG, Comar D. Regional cerebral blood flow and oxygen consumption in human aging. Stroke 1984;15(4):635–641. [PubMed: 6611613]

34. Shin W, Carroll TJ. A Self Calibrating Pulse Sequence for Real Time Quantiative Cerebral Perfusion. Proc Int Soc Magn Reson Med. 2007

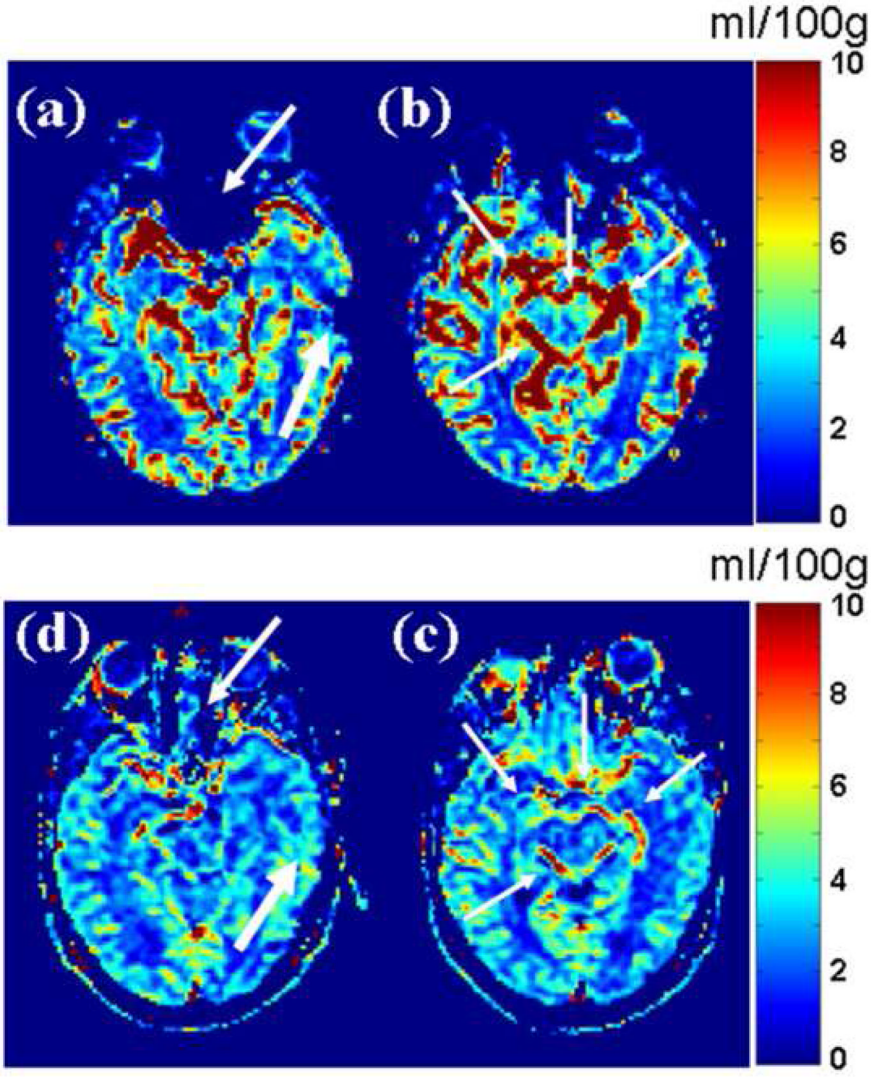

Figure 1.

A paired comparison of 2 adjacent slices of quantitative CBV (ml/100g) image slices in spin-echo and gradient echo perfusion weighted images demonstrate the benefits of SE-EPI. Images from the top row (a,b) acquired with GRE-EPI sequence (TR/TE = 1500 ms/47 ms) and the bottom row (c,d) acquired with spin-echo EPI (TR/TE = 1500 ms/60 ms/) in the same imaging session. Signal dropout near the frontal sinuses (a: thin arrows) and near a recent craniotomy (a: thick arrows). Artifact from large blood vessels is denoted with thin arrows in (b). The SE-EPI images exhibit less signal dropout and large vessel artifact. The improved image quality on the spin echo images provide better overall depiction of quantitative MR perfusion.

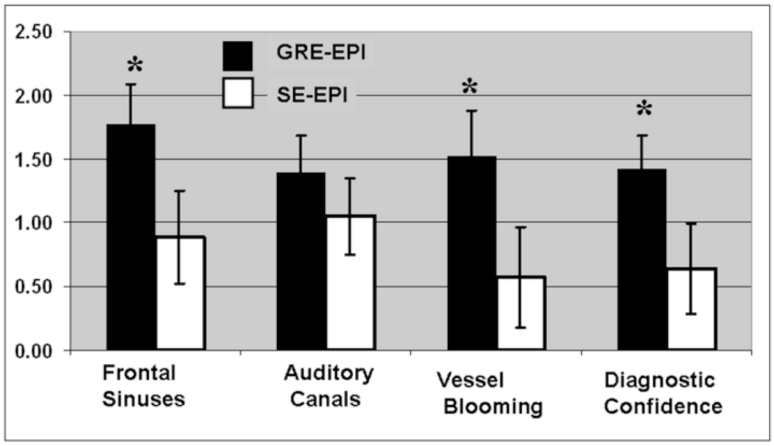

Figure 2.
Graphical results of the qualitative images analysis. Significant differences between SE-EPI and GRE-EPI are marked with an asterisks. Note that higher values (0–3) represent more artifact and less diagnostic confidence.

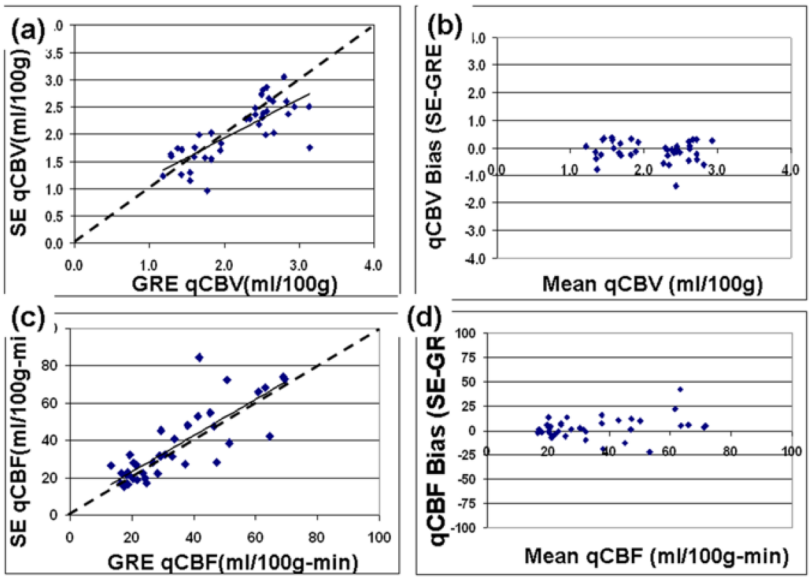

Figure 3.

Scatter plots comparing perfusion quantification from SE-EPI and GRE-EPI acquisitions in 19 patients. Correlation analysis of (a) cerebral blood volume (qCBV), and (c) cerebral blood flow (qCBF) are plotted separately. The resulting correlation fit is show as a solid line, a line of unity (y=x) are shown as dotted lines. The corresponding Bland-Altman plots (b,d) are also shown.

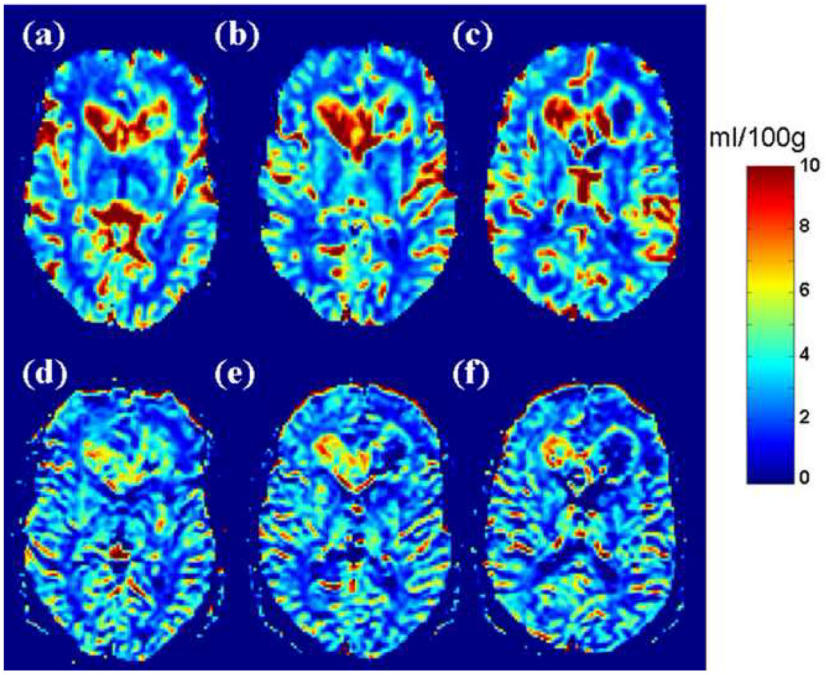

Figure 4.
A 52 year old male with “butterfly” GBM involving the genu of corpus callosum and bifrontal periventricular white matter. Both GRE-EPI (a,b,c) and SE-EPI (d,e,f) images show elevated qCBV throughout the right frontal mass and genu of corpus callosum. Increased CBV is seen at the peripheral rim of the left frontal tumor with central necrosis showing decreased qCBV seen on both GRE-EPI and SE-EPI.

Table 1

Qualitative Analysis comparing Gradient Echo EPI (GRE-EPI) and Spin –Echo EPI (SE-EPI) perfusion images. Note that for diagnostic confidence a lower score indicates higher confidence.

	GRE-EPI Mean (std)	SE-EPI Mean (std)	P-value	Kappa
Frontal sinus Artifact	1.77 (0.32)	0.89 (0.36)	<0.05	0.66
Internal Auditory Canals Artifact	1.40 (0.28)	1.05 (0.30)	0.21	0.68
Vessel “Blooming” Artifact	1.52 (0.36)	0.57 (0.40)	<0.05	0.79
Diagnostic Confidence	1.43 (0.25)	0.64 (0.36)	<0.05	0.50

Table 2

Mean values of qCBV (ml/100g) and qCBF (ml/100g-min) measured with GRE and SE-EPI. Significant differences between the SE-EPI and GRE-EPI values are marked with an asterisks.

	Spin Echo EPI		Gradient Echo EPI	
	qCBV(ml/100g)	**qCBF(ml/100g-min)**	**qCBV(ml/100g)**	**qCBF(ml/100g-min)**
White Matter	1.68 ± 0.41	22.72 ± 5.45	1.70 ± 0.38	21.02 ± 4.43
Gray Matter	2.41 ± 0.36*	50.46 ± 18.08	2.62 ± 0.28*	46.27 ± 13.67

Table 3

A comparison between SE-EPI and GRE-EPI for relative and quantitative perfusion, as determined by CBV, of pathologically confirmed high and low grade gliomas.

GRE-EPI Tumor Perfusion		
	WHO Grade II	**WHO Grades III, IV**
rCBV(A.U.)	2.98 ± 1.93	5.45 ± 3.03
qCBV(ml/100g)	4.53 ± 2.74	6.31 ± 2.93
SE-EPI Tumor Perfusion		
	WHO Grade II	WHO Grades III, IV
rCBV(A.U.)	2.59 ± 1.73	3.42 ± 0.83
qCBV(ml/100g)	4.09 ± 2.48	5.59 ± 2.11